Mechanism of affinity enhanced protein adsorption on bio-nanocapsules studied by viscoelasticity measurement with wireless QCM biosensor

Kentaro Noi[1], Masumi Iijima[2], Shun'ichi Kuroda[3], Fumihito Kato[4], and Hirotsugu Ogi[5]*

[1]*Institute for NanoScience Design, Osaka Univ., Machikaneyama 1-3, Toyonaka, Osaka 560-8531, Japan*
[2]*Department of Nutritional Science and Food Safety, Tokyo University of Agriculture, Setagaya-ku, Tokyo 156-8502, Japan*
[3]*The Institute of Scientific and Industrial Research, Osaka University, Mihogaoka 8-1, Ibaraki, Osaka 567-0047, Japan*
[4]*Department of Mechanical Engineering, Nippon Institute of Technology, 4-1 Gakuendai, Miyashiro-machi, Minamisaitama, Saitama, 345-8501, Japan*
[5]*Graduate School of Engineering, Osaka University, Yamadaoka 2-1, Suita, Osaka 565-0871, Japan*

Recent advances in functionalized bio-nanocapsules (BNCs) allow significant sensitivity enhancement in label-free biosensors. It is suggested that the sensitivity amplification is caused by higher binding affinity of BNC to target antibody. We here study the high-affinity interaction mechanism between BNC and antibody with wireless high-frequency QCM biosensors. We first confirm higher affinity between BNC and human immunoglobulin G. We then reveal that the number of the binding sites for the target antibody highly increases by immobilizing BNC molecules on the sensor surface. We finally study the change in the viscoelasticity near the sensor surface using the MEMS wireless QCM biosensor using up to 9th overtone (522 MHz). The inversely determined effective shear modulus on BNC is found to be significantly lower than the standard surface on which the receptor molecules are immobilized. We thus clarify that this surface flexibility will achieve the high affinity with the target antibody.

Japanese Journal of Applied Physics 59, SKKB03 (2020)
https://doi.org/10.35848/1347-4065/ab78e1

1. Introduction

Application of ultrasonic resonator is growing not only in gas sensor field[1–4] but also intensively in biosensors.[5–9] Biosensors detect target biomaterials by trapping them with receptor proteins immobilized on sensor surfaces. Antibodies are typical receptor proteins, among which immunoglobulin G (IgG) has been widely adopted for trapping the corresponding target proteins. Immobilization of IgG molecules on sensor surface usually requires surface modification with cross linkers such as self-assembled monolayers. The orientation control to the immobilized antibody is, however, difficult in such a case, because the Fv portion (sensing region) of IgG can face the sensor surface, being away from the targets. Using the specific binding interaction between protein A and the Fc portion of IgG, an oriented IgG immobilization was achieved by immobilizing protein A molecules first and then IgG molecules.[10,11]

A bio-nanocupsuel (BNC) has been successfully adopted to further improve the orientated immobilization of IgG molecules.[12] It exhibits many IgG-Fc-binding domains (Z domains) derived from protein A on its surface[13,14] as illustrated in Fig. 1[15] and is capable of capturing about 60 IgG molecules, orienting their Fv portions outwardly:[13,14] We refer to this BNC as ZZ-BNC. Using ZZ-BNCs on the sensor platform, detection sensitivities in label-free biosensors such as surface-plasmon-resonance biosensor and quartz-crystal-microbalance (QCM) biosensor[13] were significantly enhanced. BNCs are also used for sensitivity amplification in the sandwich assay with a QCM biosensor, which principally detects the target mass, thanks to their larger molecular mass of 6.57 MDa.[16]

Iijima *et al.*[13] reported that the sensitivity is enhanced by coating the sensor surface with ZZ-BNCs instead of protein A. This may be attributed to the increase in the number of immobilized IgG molecules, but it is also suggested that the binding affinity between IgG and ZZ-BNC becomes higher compared with that between IgG and protein A. In this paper, we study the sensitizing mechanism achieved by ZZ-BNC using high-frequency wireless QCM biosensors[17,18] through evaluation of binding affinity, number of binding site, and viscoelastisity on the sensor surface. First, we investigate the difference in the binding behavior between IgG and protein A and that between IgG and ZZ-BNC using a multichannel wireless QCM biosensor,[19] where frequency responses of the two sensor chips were simultaneously monitored. Injecting various concentration IgG solutions, we determine the number of the binding site and their binding affinity values. Second, we study the viscoelasticity change during the binding reaction using a MEMS wireless QCM biosensor[20,21] by measuring resonance-frequency changes up to 9th mode (522 MHz),[22] through which the viscoelastic parameters are inversely determined.[23,24]

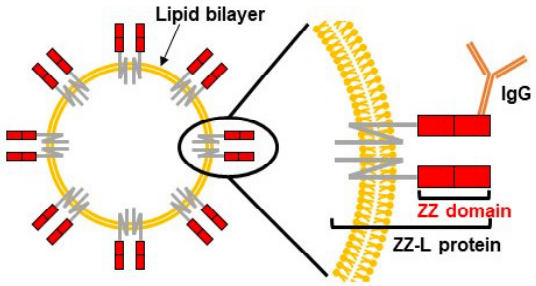

Fig. 1. Schematic structure of a ZZ-BNC.[15] A single ZZ-BNC consists of ~120 ZZ-L proteins embedded in a lipid bilayer. Each ZZ-domain terminal binds the Fc portion of an IgG molecule.

*E-mail: ogi@prec.eng.osaka-u.ac.jp

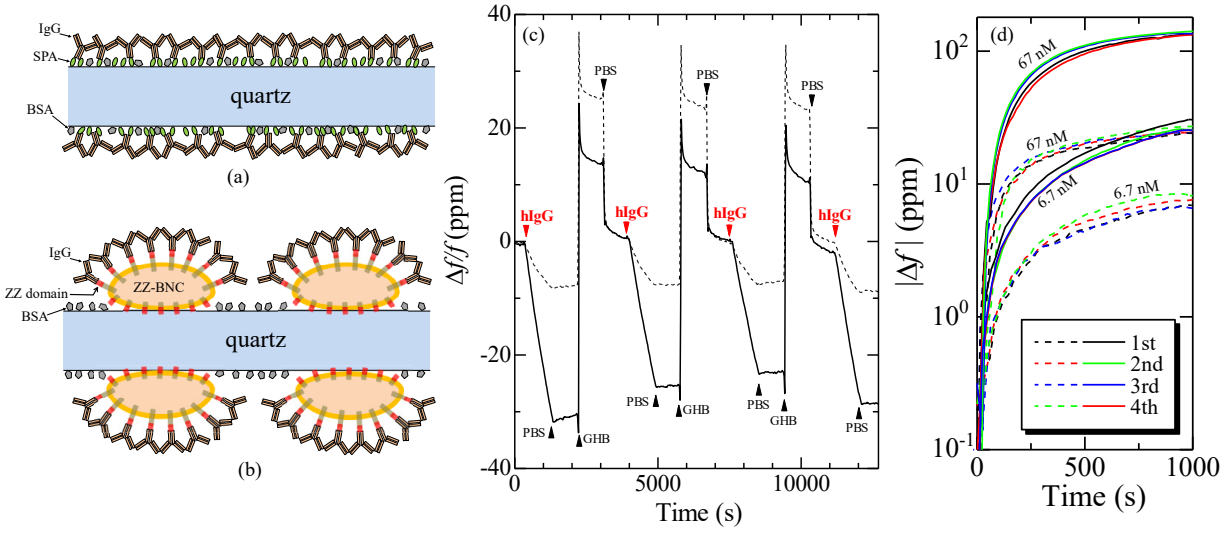

Fig. 2. (a) and (b) show illustrations near quartz surfaces when IgG molecules are captured by protein A and ZZ-BNC immobilized on the surfaces, respectively.[15] (c) Resonance-frequency changes caused by injections of 6.7-nM human IgG (hIgG), PBS solution, and glycine HCl buffer (GHB) solution.[15] Solid and broken lines denote responses on ZZ-BNC and protein-A immobilized resonators, respectively. (d) Amount of resonance-frequency changes during binding reaction with hIgG of different concentrations.[15] Solid and broken lines are responses on ZZ-BNC and protein-A immobilized resonators, respectively. Four independent measurements are shown.

.

2. Experiments

2.1 Affinity evaluation with multichannel wireless QCM

The oscillators used in the multichannel wireless QCM are AT-cut quartz plates, whose fundamental resonance frequencies are 54 MHz and 56 MHz. We deposited 5 nm Cr and then 15 nm Au thin films on both surfaces of the oscillators. Their surfaces were washed with piranha solution (98% H_2SO_4:33%H_2O_2 = 7:3) for 1 h and rinsed with ultrapure water several times. Their surfaces were cleaned with a UV ozone cleaner for 15 min. The oscillators were then immersed in 10 mM 10-carboxy-1-decanethiol solution overnight at 4 °C. After rinsing them with ethanol and ultrapure water, their surfaces were activated by 100 mM EDC (1-Ethyl-3-(3-dimethylaminopropyl) carbodiimide, hydrochloride) solution for 1 h. After rinsing them with ultrapure water, one oscillator was immersed in 20 μg/ml Staphylococcal protein A in phosphate buffered saline (PBS) solution (pH7.4), and the other oscillator was immersed in 20 μg/ml ZZ-BNC in PBS solution for 12 h at 4°C for immobilizing them. After rinsing them with ultrapure water, they were immersed in 10 mg/ml bovine-serum-albumin (BSA) solution for blocking remaining activated sites. After rinsing them with PBS solution, we set the two oscillators in the multichannel wireless QCM cell shown in Fig. 1 in Ref. 16. We then injected human IgG in PBS solutions of various concentrations at a flow rate of 100 μl/min. After each binding reaction, we injected glycine HCl buffer (GHB) solution (pH2.4) for dissociating IgG molecules from the surfaces. We repeated injections of IgG, PBS, and GHB solutions. The resonance-frequency measurement was performed by a superheterodyne spectrometer.

2.2 Viscoelasticity evaluation with MEMS wireless QCM

We prepared two MEMS wireless QCMs: One is for immobilizing protein A and the other is for immobilizing ZZ-BNC. AT-cut quartz oscillators with 58 MHz fundamental resonance frequency were packaged inside their microchannels after deposition of the 5-nm Cr and 15-nm Au thin films on both surfaces. (Details of the microchannel and its fabrication procedure are given in Ref. 21.) The immobilization procedure for protein A was the same as that used in the multichannel wireless QCM experiment. That for ZZ-BNC was slightly different; the ZZ-BNC concentration was decreased to 2 μg/ml to obtain similar resonance frequency change as that with the protein-A immobilized resonator. We injected a 6.7 nM human-IgG solution into the two MEMS QCM sensors, measuring 1st (58 MHz), 3rd (174 MHz), 5th (290 MHz), and 9th (522 MHz) resonance frequencies, simultaneously, using a vector network analyzer.

2.3 Materials and instruments

Human IgG (#16-16-090707) was purchased from Athens Research & Technology. Staphylococcal protein A (#101100) was from Invtrogen. BSA (#A3059) was from Sigma Aldrich. 10-Carboxy- decanthiol (#C385) and EDC (#W001) were from DOJINDO. The superheterodyne spectrometer (#RAM-10000) was from RITEC Inc. The vector network analyzer (#ZNB) was from Rohde & Schwarz.

3. Results and Discussion

3.1 Affinity enhancement

Figure 2(c) shows changes of the resonance frequencies during repeated injections of 6.7-nM IgG, PBS, and GHB solutions on the ZZ-BNC immobilized and protein-A immobilized resonators measured simultaneously by the multichannel wireless QCM. (Corresponding surface regions are illus-

Table I. The reaction velocity constants for association (k_a) and for dissociation (k_d), and the dissociation constant K_D for binding reactions between human IgG and ZZ-BNC and between human IgG and protein A.

	k_a ($M^{-1}s^{-1}$)	k_d (s^{-1})	K_D (nM)
IgG on ZZ-BNC	4.70×10^4	2.72×10^{-5}	0.58
IgG on protein A	5.27×10^4	9.52×10^{-5}	1.81

trated in Figs. 2(a) and (b) when IgG molecules are adsorbed on them.) Figure 2(d) shows the absolute frequency changes caused by injections of IgG solutions with two different concentrations on the two resonators. These results indicate high reproducibility of the measurements, and more importantly, it is clearly demonstrated that the ZZ-BNC immobilized resonator shows larger frequency change than the protein-A immobilized resonator in the specific binding reaction.

Figure 3 shows the frequency changes caused by IgG solutions of concentrations between 6.7 pM and 67 nM. Because the target-solution concentration, C_{IgG}, remains unchanged during its flow in a flow-injection analysis system, the binding reaction can be treated as a pseudo-first-order reaction. The resonance frequency changes exponentially in this case ($\Delta f \propto \exp(-\alpha t)$),[25] and its exponential coefficient α is expressed by $\alpha = -k_a C_{\mathrm{IgG}} + k_d$ with reaction velocity constants for adsorption k_a and that for dissociation k_d.[26] These velocity constants are determined from the relationship between α and C_{IgG},[18] and the dissociation constant K_D is then given by $K_D = k_a/k_d$. The resultant values are shown in Table I. The dissociation constant between IgG and ZZ-BNC is smaller than that between IgG and protein A by a factor of 0.3, confirming significant affinity enhancement with ZZ-BNC. With the reaction-velocity constant k_a, it is possible to evaluate the number density of the binding site, σ_0, on a sensor surface by[27]

$$\sigma_0 = \frac{\sqrt{\rho_q \mu_q}}{4 f_1^2} \frac{N_A}{p_{\mathrm{IgG}} C_{\mathrm{IgG}} k_a} \left(\frac{\mathrm{d}\Delta f}{\mathrm{d}t} \right)_{t=0} . \quad (1)$$

Here, ρ_q, μ_q, and f_1 are mass density, shear modulus, and fundamental resonance frequency of the AT-cut quartz, respectively. p_{IgG} and N_A are the molecular mass of IgG and the Avogadro constant, respectively. The inset in Fig. 3 shows the number density of the IgG binding sites on the two resonators. The ZZ-BNC coated resonator exhibits the number of biding sites significantly larger than the protein-A coated resonator by a factor about 4, indicating that a larger number of IgG molecule can be captured on ZZ-BNC, which contributes to the sensitivity enhancement.

3.2 *Viscoelasticity calculation*

For investigating the mechanism of higher affinity with ZZ-BNC, we evaluate the viscoelasticity change near the surface region during the binding reaction. We adopt a three continuous layer model, consisting of the quartz layer (elastic material), protein layer (Kelvin-Voigt medium), and the water layer (Newtonian fluid),[28–30] and inversely calculated changes of the layer thickness (h_p), the viscosity (η_p), and the shear modulus (μ_p) of the protein layer using four measurements of 1st, 3rd, 5th, and 9th resonance frequencies. Because the protein layer contains the surrounding solution in actuality, the thickness, viscosity, and shear modulus of the protein layer

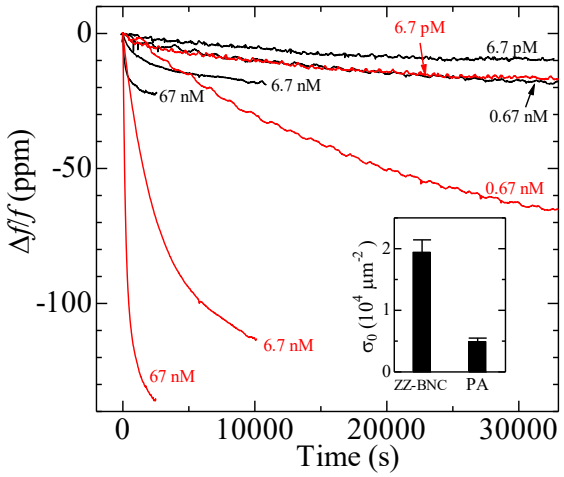

Fig. 3. Resonance frequency changes caused by injections of IgG solutions of various concentrations observed by the ZZ-BNC immobilized resonator (red) and the protein-A immobilized resonator (black). The inset shows the number of binding site on the two resonators.

are not exactly the same as those of the protein itself, and we refer to them as effective thickness, effective viscosity, and effective shear modulus. Details of the inverse calculation appear in our previous studies.[22,24]

Figures 4(a) and (c) show the resonance frequency changes during the flow of the 6.7-nM IgG solution on the ZZ-BNC immobilized resonator and the protein-A immobilized resonator, respectively. For making fair comparison, we immobilized ZZ-BNCs with the lower concentration solution, so that the resonance-frequency change of the fundamental mode becomes comparable between the two resonators. However, significant difference appears in higher modes; although 1st to 5th modes show similar frequency changes for the protein-A coated resonator, the higher modes show different frequency changes from the fundamental mode for the ZZ-BNC coated resonator. A higher-mode resonance-frequency change is expected to be smaller with a softer material because the deformation fails to follow the fast surface movement. Figures 4(b) and (d) show inversely determined effective thickness, effective viscosity, and effective shear modulus of the protein layer for the ZZ-BNC and protein-A coated resonators, respectively. As presented in Fig. 4(b), the ZZ-BNC surface keeps smaller shear modulus and higher viscosity, whereas as shown in Fig. 4(d) the protein-A surface becomes stiffer in a short time with capturing IgG molecules accompanied by significant viscosity decrease. Thus, this result indicates that the protein layer formed on protein A molecules becomes rigid, and we consider that this will be caused by the interaction among the captured IgG molecules. On such a rigid platform, the surface stress due to adsorption of IgG will enhance the detachment of IgG molecules, so that the apparent k_d value will increase compared with thermodynamically ideal k_d value. On the other hand, the softened BNC platform will release the surface stress, and nearly ideal k_d value is realized, keeping the high affinity. The rotational Brownian motion was observed for an IgG molecule attached on ZZ-BNC,[14] which supports our view that the flexibility of the ZZ-BNC platform

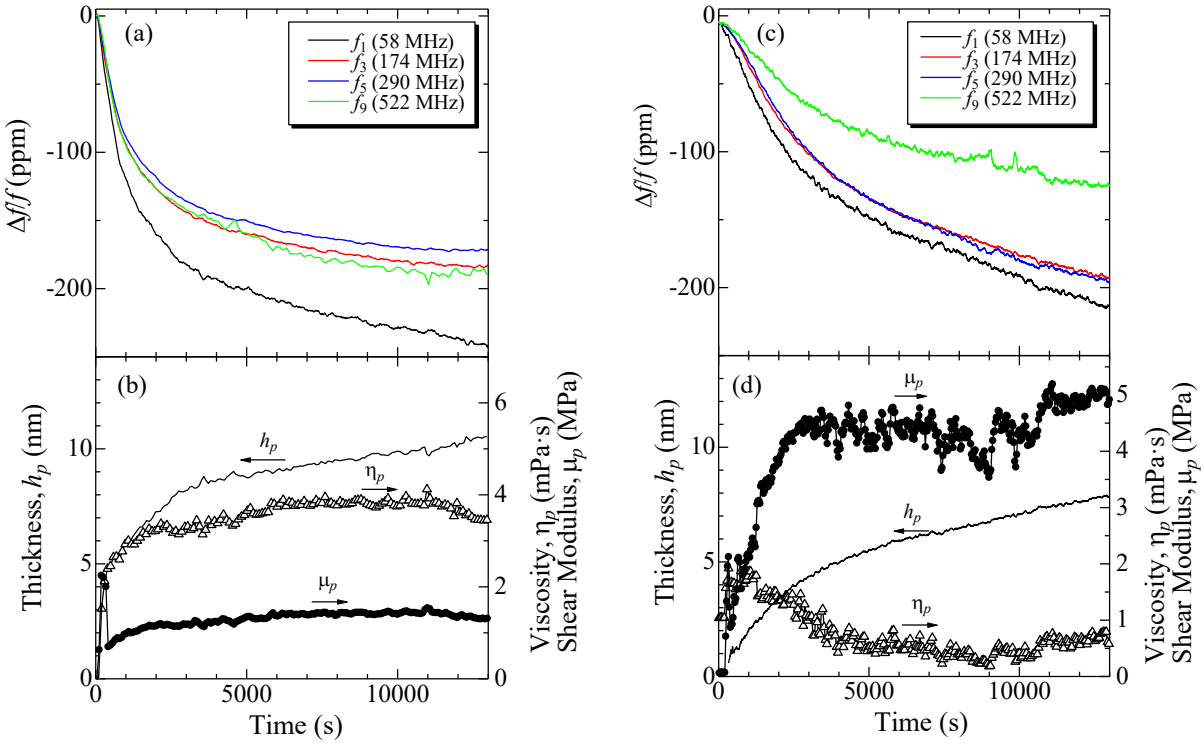

Fig. 4. (a) Changes of 1st, 3rd, 5th, and 9th resonance frequencies caused by injection of 6.7 nM IgG solution on ZZ-BNC immobilized MEMS QCM, and (b) inversely calculated effective thickness h_p, effective viscosity η_p, and effective shear stiffness μ_p of the formed protein layer. (b) Changes of the four resonance frequencies caused by injection of 6.7 nM IgG solution on the protein-A immobilized MEMS QCM, and (b) inversely calculated h_p, viscosity η_p, and μ_p values.

remains even after IgG adsorption. The k_a value on the ZZ-BNC layer is close to that on the protein-A layer (Table I), indicating that k_a is less sensitive to the surface stress, because it depends on the strength of the chemical (or electrostatic) interaction between the pairs when they approach each other.

4. Conclusion

Binding reaction between IgG and ZZ-BNC is studied by wireless multichannel QCM biosensor and wireless MEMS-QCM biosensor. First, it is confirmed that binding affinity is enhanced by using ZZ-BNC instead of protein A despite that IgG molecules are captured by the same binding domains. Second, the number of the IgG binding site was evaluated, which is larger on ZZ-BNCs than on protein A molecules by a factor of 4. Third, the viscoelasticity change was evaluated during the binding reaction of IgG molecules. The IgG layer formed on protein A molecules becomes significantly rigid during the adsorption reaction, which will induce the in-plane residual stress and increase the reaction-velocity constant for dissociation k_d. The IgG layer formed on ZZ-BNCs, on the other hand, remains softened state, which relaxes the in-plane stress and remains k_d value smaller, resulting in higher affinity in the binding reaction.

Acknowledgement

This study was supported by Development of Advanced Measurement and Analysis Systems from Japan Science and Technology Agency (pro ject no. JP- MJSN16B5).

1) W. P. Jakubik, M. W. Urbanczyk, S. Kochowski, and J. Bodzenta: Sens. Actuators, B 82, 265 (2002).
2) K. Yamanaka, S. Akao, N. Takeda, T. Tsuji, T. Oizumi, H. Fukushi, T. Okano, and Y. Tsukahara: Jpn. J. Appl. Phys. 58, SGGB04 (2019).
3) L. Zhou, N. Nakamura, A. Nagakubo, and H. Ogi: Appl. Phys. Lett. 115, 171901 (2019).
4) N. Nakamura, T. Ueno, and H. Ogi: Appl. Phys. Lett. 114, 201901 (2019).
5) F. Höök, B. Kasemo, T. Nylander, C. Fant, K. Sott, and H. Elwing: Anal. Chem. 73, 5796 (2001).
6) M. P. Jonsson, P. Jönsson, and F. Höök: Anal. Chem. 80, 7988 (2008).
7) P. Ding, R. Liu, S. Liu, X. Mao, R. Hu, and G. Li: Sens. Actuators, B 188, 1277 (2013).
8) Y. Zhang, J. Luo, A. J. Flewitt, Z. Cai, and X. Zhao: Biosens. Bioelectron. 116, 1 (2018).
9) F. Kato, H. Noguchi, Y. Kodaka, N. Oshida, and H. Ogi: Jpn. J. Appl. Phys. 57, 07LD14 (2018).
10) D. M. Gersten and J. J. Marchalonis: J. Immunol. Methods. 24, 305 (1978).
11) L. Björck and G. Kronvall: J. Immunol. 133, 969 (1984).
12) M. Iijima, S. Kuroda: Biosens. Bioelectron. 89 810 (2017).
13) M. Iijima, H. Kadoya, S. Hatahira, S. Hiramatsu, G. Jung, A. Martin, J. Quinn, J. Jung, S.-Y. Jeong, E. K. Choi, T. Arakawa, F. Hinako, M. Kusunoki, N. Yoshimoto, T. Niimi, K. Tanizawa, and S. Kuroda: Biomaterials 32, 1455 (2011).
14) M. Iijima, M. Somiya, N. Yoshimoto, T. Niimi, and S. Kuroda: Sci. Rep. 2, 790 (2012).
15) K. Noi, M. Iijima, S. Kuroda, and H. Ogi, Proc. 40th Symp. Ultrason. Electron. 40, 3P2-12 (2019).
16) K. Noi, M. Iijima, S. Kuroda, and H. Ogi: Sens. Actuat. B: Chem. : 293, 59 (2019).
17) H. Ogi, H. Nagai,Y. Fukunishi, M. Hirao, and M. Nishiyama: Anal. Chem. 81,8068 (2009).
18) K. Noi, A. Iwata, F. Kato, and H. Ogi: Anal. Chem. 91, 9398 (2019).

19) H. Ogi, H. Nagai,Y. Fukunishi, T. Yanagida, M. Hirao, and M. Nishiyama: Anal. Chem. 82, 3957 (2010).
20) F. Kato, H. Ogi, T. Yanagida, S. Nishikawa, M. Nishiyama, and M. Hirao: Jpn. J. Appl. Phys. 50, 07HD03 (2011).
21) F. Kato, H. Ogi, T. Yanagida, S. Nishikawa, M. Hirao, and M. Nishiyama: Biosen. Bioelectron. 33, 139 (2012).
22) Y.-T. Lai, H. Ogi, K. Noi, and F. Kato: Langmuir 34, 5474 (2018).
23) T. Shagawa, H. Torii, F. Kato, H. Ogi, and M. Hirao: Jpn. J. Appl. Phys. 54, 068001 (2015).
24) T. Shagawa, H. Torii, F. Kato, H. Ogi, and M. Hirao: Jpn. J. Appl. Phys. 54, 096601 (2015).
25) C. Y. Liu, X. Yu, R. Zhao, D. Shangguan, Z. Bo, and G. Liu: Biosens. Bioelectron. 19, 9 (2003).
26) H. Ogi, K. Motohisa, K. Hatanaka, T. Ohmori, M. Hirao, and M. Nishiyama: Biosens. Bioelectron. 22, 3238 (2007).
27) H. Ogi, Y. Fukunishi, H. Nagai, K. Okamoto, Masahiko Hirao, and M. Nishiyama: Biosens. Bioelectron. 24, 3148 (2009).
28) C. Reed, K. Kanazawa, and J. H. Kaufman: J. Appl. Phys. 68, 1993 (1990).
29) M. V. Voinova, M. Jonson, and B. Kasemo: J. Phys.: Condens. Matter 9, 7799 (1997).
30) M. V. Voinova, M. Rodahl, M. Jonson, and B. Kasemo, Phys. Scr. 59, 391 (1999).